Single-Epoch GNSS Array Integrity: An Analytical Study

A. Khodabandeh and P.J.G. Teunissen

Abstract

In this contribution we analyze the integrity of the GNSS array model through the so-called uniformly most powerful invariant (UMPI) test-statistics and their corresponding minimal detectable biases (MDBs). The model considered is characterized by multiple receivers/satellites with known coordinates where the multi-frequency carrier-phase and pseudo-range observables are subject to atmospheric (ionospheric and tropospheric) delays, receiver and satellite clock biases, as well as instrumental delays. Highlighting the role played by the model's misclosures, analytical multivariate expressions of a few leading test-statistics together with their MDBs are studied that are further accompanied by numerical results of the three GNSSs GPS, Galileo and BeiDou.

Keywords

Array model • GNSS misclosures • Integrity • Minimal detectable bias (MDB) • Uniformly most powerful invariant (UMPI) test-statistic

1 Introduction

The notion of the GNSS array model, here, refers to an array of antennas tracking the multi-frequency carrier-phase/pseudo-range observables in the presence of atmospheric effects. The coordinates of antennas and satellites are assumed to be known. The definition presented is rather general in the sense that even the medium-scale control networks can also be considered as an array. Examples of such are the continuously operating reference station (CORS) networks sending corrections to the RTK- and/or PPP-RTK users (de Jonge 1998; Odijk et al. 2014), a set of antennas mounted on rigid platforms improving the position/attitude of points in its vicinity (Teunissen 2010, 2012), and the ground based augmentation systems (GBASs) supporting safe flight procedures such as landing, departure and surface operations at an airport (Khanafseh et al. 2012; Giorgi et al. 2012). Despite their different applications, all of the aforementioned arrays are, however, utilized for the purpose of the *same* functionality, that is, providing accurate corrections for the users. Ensuring the integrity and reliability of the corrections, even at the pre-analysis level, is therefore of great importance, see e.g., Teunissen (1998); Teunissen and de Bakker (2012).

Integrity monitoring and quality control of the GNSS array model is the topic of this contribution. We confine our study to the *single-epoch* scenario as it is indeed the ultimate goal of the near real-time applications and, at the same time, brings us conservative thresholds of the reliability measures of the corresponding multi-epoch scenario. Our strategy commences with the model's misclosures. Although the GNSS misclosures can be treated as diagnostic tools in

A. Khodabandeh (✉)
Department of Spatial Sciences, GNSS Research Centre, Curtin University of Technology, Perth, WA 6845, Australia
e-mail: amir.khodabandeh@curtin.edu.au

P.J.G. Teunissen
Department of Spatial Sciences, GNSS Research Centre, Curtin University of Technology, Perth, WA 6845, Australia

Department of Geoscience and Remote Sensing, Delft University of Technology, Delft, The Netherlands
e-mail: p.teunissen@curtin.edu.au

International Association of Geodesy Symposia,
DOI 10.1007/1345_2015_64,

their own right, we make use of certain linear functions of them to formulate the UMPI test-statistics which give rise to the highest probability of the detection for a class of critical regions. For an overview of the underlying principles of the UMPI test, see Arnold (1981), and for its applications to hypothesis testing in linear models, see e.g. Teunissen (2000).

The test-statistics to be studied are (1) the array-, antenna- and satellite-detectors in which the overall/local validity of the model is tested, (2) the celebrated w-test-statistic for the purpose of outlier identification and (3) the atmospheric detectors well suited to the small-scale arrays. The detectability of the tests is formulated via the corresponding MDBs where the associated numerical illustrations, emphasized on the three GNSSs GPS, Galileo and BeiDou, are also given.

2 Array Model and the GNSS Misclosures

Consider a single antenna, say antenna r ($r = 1, \ldots, n$), that tracks s number of commonly-viewed satellites on frequency j ($j = 1, \ldots, f$). One can then put the corresponding *undifferenced* carrier-phase observations on each frequency, as the s-vectors $\phi_{r,j}$ ($j = 1, \ldots, f$), into a higher-dimensioned vector $\phi_r = [\phi_{r,1}^T, \ldots, \phi_{r,f}^T]^T$. Doing the same to the pseudo-range observations p_r and collecting observations of all n antennas, the final $sf \times n$ matrices of carrier-phase and pseudo-range data of the array can be, respectively, formulated as

$$\Phi = [\phi_1, \ldots, \phi_n], \quad P = [p_1, \ldots, p_n]$$

The satellite-/receiver-dependent biases are, respectively, canceled out by applying the between-receiver single-differenced (SD) operator D_n and the between-satellite SD operator D_s (Teunissen 1997). The multivariate representation of the double-differenced (DD) observation equations of the array model, under the null hypothesis H_o, reads then

$$\begin{aligned}
\mathsf{E}\{(I_f \otimes D_s^T)\Phi\ D_n\} &= (e_f \otimes D_s^T g)\ \tau^T D_n - (\mu \otimes I_{s-1}) \\
&\quad \times D_s^T\, \iota\ D_n + (\Lambda \otimes I_{s-1})\ Z \\
\mathsf{E}\{(I_f \otimes D_s^T)P\ D_n\} &= (e_f \otimes D_s^T g)\ \tau^T D_n + (\mu \otimes I_{s-1}) \\
&\quad \times D_s^T\, \iota\ D_n
\end{aligned} \tag{1}$$

$$\begin{aligned}
\mathsf{D}\{vec[(I_f \otimes D_s^T)\Phi\ D_n]\} &= D_n^T D_n \otimes Q_\phi \otimes D_s^T W_s^{-1} D_s \\
\mathsf{D}\{vec[(I_f \otimes D_s^T)P\ D_n]\} &= D_n^T D_n \otimes Q_p \otimes D_s^T W_s^{-1} D_s
\end{aligned} \tag{2}$$

where the s-vector g contains functions mapping the slant tropospheric delays (STDs) onto the zenith tropospheric delays (ZTDs) $\tau = [\tau_1, \ldots, \tau_n]^T$. The $s \times n$ matrix ι is introduced as $\iota = [\iota_1, \ldots, \iota_n]$, with ι_r being the s-vector of the (first-order) slant ionospheric delays of antenna r. The f-vector μ contains the ionospheric coefficients $\mu_j = \lambda_j^2/\lambda_1^2$, with λ_j being the wavelengths positioned on the $f \times f$ diagonal matrix Λ. The matrix Z contains the integer-valued DD ambiguities. The $f \times f$ positive-definite matrices Q_ϕ and Q_p are the cofactor matrices of the phase and pseudo-range observable-type. The $s \times s$ diagonal matrix W_s captures the satellite elevation dependency of the observations. I and e, respectively, denote the identity matrix and the vector of ones, where the subscripts indicate their size. The operator $\otimes$ denotes the Kronecker product. $\mathsf{E}\{.\}$ and $\mathsf{D}\{.\}$ are the mathematical expectation and dispersion operators, respectively. The operator $vec[.]$ vectorizes the associated matrix.

Using model (1) and (2), we are interested to check the validity of the model against unaccounted effects. To do so, we therefore work with the conditioned equations of (1) and the corresponding misclosures. The idea to employ the conditioned equations rather than the commonly-used observation equations is motivated by the desire to characterize the intrinsic behavior of the array model in relation to the possible misspecifications. This is indeed realized by forming the GNSS misclosures showing the contribution of the observations to the redundancy of the model.

2.1 GNSS-Based Decoupled Misclosures

Although the misclosures of (1) can be formed in many different ways, we form those that are group-wise *uncorrelated* and at the same time have easy interpretations. The GNSS-based decoupled misclosures, in case of the ambiguity-float scenario, are introduced as follows (cf. Appendix)

$$\begin{aligned}
&\textit{i: Frequency-differenced misclosures:} \\
&M_1 = [(D_f^T \mu)^{\perp T} D_f^T \otimes c_{d|\tau}^2 \bar{g}^T W_s]\ P\ D_n \\
&\textit{ii: Atmosphere-free misclosures:} \\
&M_2 = [\mu^{\perp T} \otimes (D_s^T g)^{\perp T} D_s^T]\ P\ D_n
\end{aligned} \tag{3}$$

where $(.)^\perp$ denotes the orthogonal complement basis matrix. We introduce the s-vector $\bar{g} = g + (c_{d\tau}/c_\tau^2)e_s$, in which the satellite-domain (co)variance-type scalars $c_{d|\tau}^2$, $c_{d\tau}$ and c_τ^2 are computed as

$$\begin{aligned}
c_\tau^2 &= \frac{e_s^T W_s e_s}{[e_s^T W_s e_s][g^T W_s g] - [g^T W_s e_s]^2} \\
c_{d\tau} &= \frac{-g^T W_s e_s}{[e_s^T W_s e_s][g^T W_s g] - [g^T W_s e_s]^2}, \quad c_{d|\tau}^2 = \frac{1}{e_s^T W_s e_s}
\end{aligned} \tag{4}$$

With regard to (3), M_1 and M_2, respectively, contribute to the model's redundancy of size $(f-2)$ and $(f-1)(s-2)$ per baseline. After fixing ambiguities, similar expressions can be obtained for the phase and phase-and-code misclosures.

2.2 Atmosphere-Aided Decoupled Misclosures

The GNSS-based misclosures, presented in (3), contain the *complete* information needed to check and to study the quality of the observation matrices Φ and P in (1). One may, however, strengthen the model by using a-priori atmospheric information, i.e. the spatial dependency of the atmospheric delays. In case of not-too-large arrays, the differential atmospheric delays, with amount of uncertainty, would thus play the role of pseudo-observables as

$$\begin{aligned} &\mathsf{E}\{D_s^T\iota\ D_n\}=D_s^T\iota\ D_n, \text{ with } \mathsf{D}\{D_s^T\iota\ D_n\}=\sigma_\iota^2\ D_n^T D_n\otimes D_s^T W_s^{-1} D_s \\ &\mathsf{E}\{D_n^T\tau\} = D_n^T\tau, \qquad \text{with } \mathsf{D}\{D_n^T\tau\} = \sigma_\tau^2\ D_n^T D_n \end{aligned} \tag{5}$$

with σ_ι^2 and σ_τ^2 being the a-priori ionospheric and tropospheric variances, respectively.

Appending the preceding equations to (1) does increase the redundancy of the model by comparing the GNSS-based estimators of the differential atmospheric delays with their pseudo-observable ones (s redundant observations per baseline). This, in a similar way to (3), provides us with the atmosphere-aided misclosures.

3 UMPI Test-Statistics and Their MDBs

Given the GNSS decoupled misclosures introduced in the previous section, we are now in a position to form various test-statistics.

Theorem 1 (UMPI Test-Statistic and Its MDB) *Let the alternative hypothesis H_a be related to the null hypothesis H_o as $\mathsf{E}\{vec[Y]|H_a\} = \mathsf{E}\{vec[Y]|H_o\} + C_Y\nabla$, where the q-vector of misspecifications ∇ is linked to the observations by the full-rank design matrix C_Y. Given a representation for the model's misclosures as $M = B^T vec[Y]$ under H_o, the UMPI test-statistic T_q and its MDB are respectively given by*

$$T_q = \frac{tr\{Q_{MM}^{-1} P_{C_M} M M^T\}}{tr\{P_{C_M}\}} \tag{6}$$

$$||\nabla|| = \sqrt{\frac{v_{q,\alpha,\gamma}}{d_Y^T C_M^T Q_{MM}^{-1} C_M d_Y}}, \quad \nabla = ||\nabla|| d_Y \tag{7}$$

where $Q_{MM} = \mathsf{D}\{M\}$ and $C_M = B^T C_Y$, with the projector $P_{C_M} = C_M(C_M^T Q_{MM}^{-1} C_M)^{-1} C_M^T Q_{MM}^{-1}$. The scalar $v_{q,\alpha,\gamma}$ is the χ^2-noncentrality parameter to be determined by the power of the test γ and the probability of false alarm α. The operator $tr\{.\}$ denotes the trace of a matrix, whereas $||.||^2 = (.)^T(.)$ is the squared-norm of a vector.

Proof see Appendix. □

The above theorem shows how the multivariate representation of the UMPI test-statistic is realized through the model's misclosures and the type of misspecifications, i.e. C_Y. We remark that the test-statistic T_q follows central and noncentral F-distribution under H_o and H_a, respectively, that is, $T_q|H_o \sim F(q,\infty,0)$ and $T_q|H_a \sim F(q,\infty,v)$, with the first two arguments q, ∞ being the degrees of freedom and v the noncentrality parameter.

As to the GNSS array model, one may formulate a rather general structure for the misspecification design matrix C_Y at the *undifferenced* level. The following structure has been adopted in this study

$$\mathsf{E}\{\tilde{Y}|H_a\} = \mathsf{E}\{\tilde{Y}|H_o\} + (C_f \otimes C_s)\ \nabla\ C_n^T \tag{8}$$

where the full-rank matrices C_f, C_s and C_n specify the type of misspecification ∇ in the frequency-, satellite- and antenna-domain, respectively. The role of the *atmosphere-corrected* observation matrix $\tilde{Y}$ can be taken by $\tilde{P}$ and $\tilde{\Phi}$ or both of them, in which we define

$$\begin{aligned} \tilde{P} &= P - (e_f \otimes g)\tau - (\mu \otimes I_s)\iota \\ \tilde{\Phi} &= \Phi - (e_f \otimes g)\tau + (\mu \otimes I_s)\iota \end{aligned} \tag{9}$$

MDB-Parametrization In general there is no unique solution for the MDB of the misspecifications of a *multi dimensional* type. This issue can be properly circumvented through an MDB-parametrization as follows

$$\nabla = ||vec[\nabla]||\ (d_f \otimes d_s)\ d_n^T \tag{10}$$

with d_f, d_s and d_n being, respectively, the frequency-, satellite- and antenna-domain vectors such that their resultant vector $d_n \otimes d_f \otimes d_s$ is of length 1, i.e. a direction vector.

In the following, a few important test-statistics, together with their MDBs, will be specialized by setting C_f, C_s and C_n in (8) to certain structures.

3.1 Array-, Antenna- and Satellite-Detectors

First one needs to check the validity of the array model against any type of misspecification that might potentially occur. The stated validity can be either of an *overall* type

or of a *local* type. The overall validity of the model is tested through the array-detector characterized by the following setting

$$\textit{array-detector:} \quad C_f \mapsto I_f, \quad C_s \mapsto D_s, \quad C_n \mapsto D_n \tag{11}$$

Depending on the a-priori atmospheric variances σ_ι^2 and σ_τ^2, several expressions can be formulated. In case of atmosphere-fixed scenario, i.e. $\sigma_\iota^2 = 0$ and $\sigma_\tau^2 = 0$, the array-detector can be shown to take the following form (cf. Appendix)

$$\begin{aligned} T_q = &\frac{1}{q} tr\{[Q_p^{-1} \otimes W_s P_{e_s}^{\perp}]\, \tilde{P}\, P_{D_n} \tilde{P}^T\} \\ &+ \frac{1}{q} tr\{[Q_\phi^{-1} \otimes W_s P_{e_s}^{\perp}]\, \tilde{\Phi}\, P_{D_n} \tilde{\Phi}^T\} \end{aligned} \tag{12}$$

with the projectors $P_{e_s}^{\perp} = I_s - c_{d|\tau}^2 e_s e_s^T W_s$ and $P_{D_n} = I_n - (1/n) e_n e_n^T$. The degrees of freedom q is determined upon choosing the following scenarios

$$\begin{aligned} &\textit{codeless data } (Q_p^{-1} = 0): \Rightarrow q = f(s-1)(n-1) \\ &\textit{phaseless data } (Q_\phi^{-1} = 0): \Rightarrow q = f(s-1)(n-1) \\ &\textit{code+phase data}: \Rightarrow q = 2f(s-1)(n-1) \end{aligned} \tag{13}$$

The corresponding MDB, in accordance with (7), reads

$$||vec[\nabla]|| = \frac{\nu_{q,\alpha,\gamma}^{\frac{1}{2}}}{\sqrt{[d_f^T (Q_p^{-1} + Q_\phi^{-1}) d_f][d_s^T D_s^T W_s P_{e_s}^{\perp} D_s d_s][d_n^T D_n^T P_{D_n} D_n d_n]}} \tag{14}$$

Clearly a judgment on the size of the MDB cannot be easily made since it depends on the three vectors d_f, d_s and d_n. Keeping fixed two vectors out of which however, one can still gain information on the sensitivity of the MDB to the contributing factors like the number of frequencies/satellites and the quality of the observables. This idea leads to locally validate the model by testing observations of a particular antenna and/or those of a particular satellite. We can therefore characterize the antenna-/satellite-detector upon the following setting

$$\begin{aligned} &\textit{antenna-detector:} \quad C_f \mapsto I_f, \quad C_s \mapsto D_s, \quad C_n \mapsto u_r^n \\ &\textit{satellite-detector:} \quad C_f \mapsto I_f, \quad C_s \mapsto u_i^s, \quad C_n \mapsto D_n \end{aligned} \tag{15}$$

where u_r^n denotes the canonical n-vector containing zeros except the r^{th} element equal to one. The canonical vector u_i^s is defined similarly. With this setting, in an analogous way to (11) and (12), expressions of the stated test-statistics as well as their MDBs can be obtained. For the atmosphere-fixed case, the degrees of freedoms of the antenna-/satellite-detector are $q = f(s-1)$ and $q = f(n-1)$, respectively.

3.2 *w*-Test-Statistic and the MDB of Single Outliers

We now focus our attention to the well-known w-test-statistic employed for the purpose of identification of a single erroneous observation (Baarda 1968). The structure of C_Y is then set to

$$\textit{w-test-statistic:} \quad C_f \mapsto u_j^f, \quad C_s \mapsto u_i^s, \quad C_n \mapsto u_r^n \tag{16}$$

Similar to the array-detector, depending on the scenarios considered, several expressions can be given to the w-test-statistic. The structures of the corresponding MDB do however follow the same pattern. Let us, for the moment, consider STDs rather than ZTDs in the model. The code-outlier MDB can be shown to read as

$$\begin{aligned} ||vec[\nabla]||_{STD} = &\nu_{1,\alpha,\gamma}^{\frac{1}{2}} \times [\tfrac{n}{n-1}]^{\frac{1}{2}} \times [w^i (1 - [\tfrac{w^i}{\bar{w}}]\tfrac{1}{s})]^{-\frac{1}{2}} \\ &\times [\tfrac{\sigma_{p_j}^2}{1 - (\sigma_{\hat{p}_j}^2 / \sigma_{p_j}^2)}]^{\frac{1}{2}} \end{aligned} \tag{17}$$

Four contributing elements show up themselves in the above MDB that are described in the following:

Noncentrality Parameter $\nu_{1,\alpha,\gamma}$ Given the fixed probability of false alarm α, the χ^2-noncentrality parameter increases as the power of the test γ increases. In other words, for a given fixed model and a fixed α, the higher the power of the test is sought, the larger the MDB becomes.

Antenna-Specific Part $[n/(n-1)]^{\frac{1}{2}}$ This clearly shows that an increase in the number of antennas n could decrease the size of the outlier MDB considerably, would one, in the beginning, consider a *limited* number of antennas (e.g. $n = 2$ or $n = 3$). However, the stated MDB *does not* significantly decrease in size by adding an extra antenna when dealing with an array of a *large* number of antennas.

Satellite-Specific Part $[w^i (1 - [\frac{w^i}{\bar{w}}]\frac{1}{s})]^{-\frac{1}{2}}$ This term depends on three factors, namely, 1) the elevation-dependent weight w^i of an individual satellite, say i, 2) the mean value of w^i ($i = 1, \ldots, s$) denoted by $\bar{w}$, and 3) the number of common satellites s. In this study, we make use of the exponential elevation weighting strategy to form the diagonal

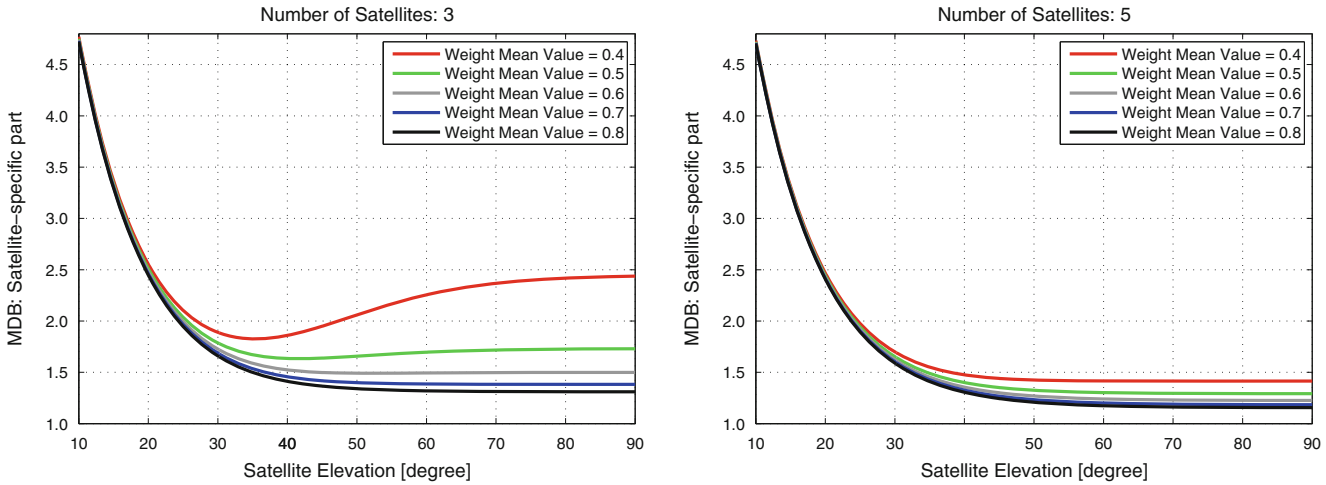

Fig. 1 Satellite-specific part of the outlier MDBs as function of the satellite elevation for different satellite configuration. The overall satellite configuration has been characterized by the weight mean value '$\bar{w}$'

elements of matrix W_s, i.e. w^i (Euler and Goad 1991)

$$w^i = [1 + 10\exp(-\frac{\epsilon^i}{10^\circ})]^{-2}, \quad i = 1, \ldots, s \tag{18}$$

where ϵ^i is the elevation of satellite i [degree] with respect to the reference antenna. Note that the elevation-dependent weight w^i should not be confused with the w-test-statistic.

Figure 1 depicts the satellite-specific part as function of the elevation of an individual satellite. The graphs have been presented for different values of $\bar{w}$ reflecting the overall configuration of the satellites with respect to the array ($0.4 \leq \bar{w} \leq 0.8$). This has been done for two cases, the case where the number of satellites is $s = 3$ (left-panel) and the other one with $s = 5$ (right-panel). As shown, the size of the MDB of an outlier, occurred in a single observation of satellites of *low elevation* (e.g. $10^\circ \leq \epsilon^i \leq 20^\circ$), is governed by the elevation of the corresponding satellite only, irrespective of the number/configuation of the satellites. In case of satellites of a higher elevation, the scenario would change as the number of satellites starts taking an active role as well. Considering a limited number of common satellites, it is interestingly observed that the MDB does not *generally* decrease as the elevation of the corresponding satellite increases (see the red thick line in Fig. 1, left-panel). In this case, in addition to the satellite elevation, the overall satellite configuration would also contribute to the size of the MDB. The stated contribution does however get insignificant once the number of satellite increases (see Fig. 1, right-panel). In the situations where the number of satellites is large enough (e.g. more than 5), one can therefore simply consider the elevation of each satellite *individually* to analyze the corresponding outlier MDB.

Frequency-Specific Part $[\sigma^2_{p_j}/(1 - (\sigma_{\hat{p}_j}/\sigma_{p_j})^2)]^{\frac{1}{2}}$ In addition to the variance of an individual pseudo-range observable-type $\sigma^2_{p_j}$, this term is also dependent on the variance of the *adjusted* observable-type denoted by $\sigma^2_{\hat{p}_j}$. This quantity in turn is a function of the a-priori atmospheric variances, the quality of the other pseudo-range observable-types through Q_p and the ionospheric vector μ.

Figure 2 shows the frequency-specific part as function of the inter-station distance for the three GNSSs GPS, Galileo and BeiDou. In order to link the inter-station distance to the ionospheric variance σ^2_ι, use has been made of that given in Schaffrin and Bock (1988). The graphs have been plotted for the troposphere-fixed case $\sigma^2_\tau = 0$ (top-panel) as well as the troposphere-float case $\sigma^2_\tau \to \infty$ (bottom-panel). As shown, the frequency-specific part behaves almost unchanged up to a certain inter-station distance (in this study around 100 [km]). In contrast to the single-frequency data (red dots), the MDB associated with the multi-frequency data does not significantly change as the inter-station distance increases (troposphere-fixed case). Because of the dispersive nature of the ionospheric effects (i.e. dependency on the frequencies), the *GNSS-based* misclosures would, in addition to the atmosphere-aided ones, also contribute to the w-test-statistic, whereas they do vanish in case of single-frequency data (cf. (3)). It is also important to note that there is no redundancy in the single-frequency troposphere-float scenario, thus giving rise to infinite MDBs. The single-frequency case is therefore excluded from the graphs of the bottom-panel. We remark, due to a generally better precision of the Galileo's signals, that the associated results illustrate a superior performance to those of GPS and BeiDou. The pseudo-range zenith-referenced standard deviation is taken as 25 [cm] for GPS/BeiDou, and as 20 [cm] for Galileo .

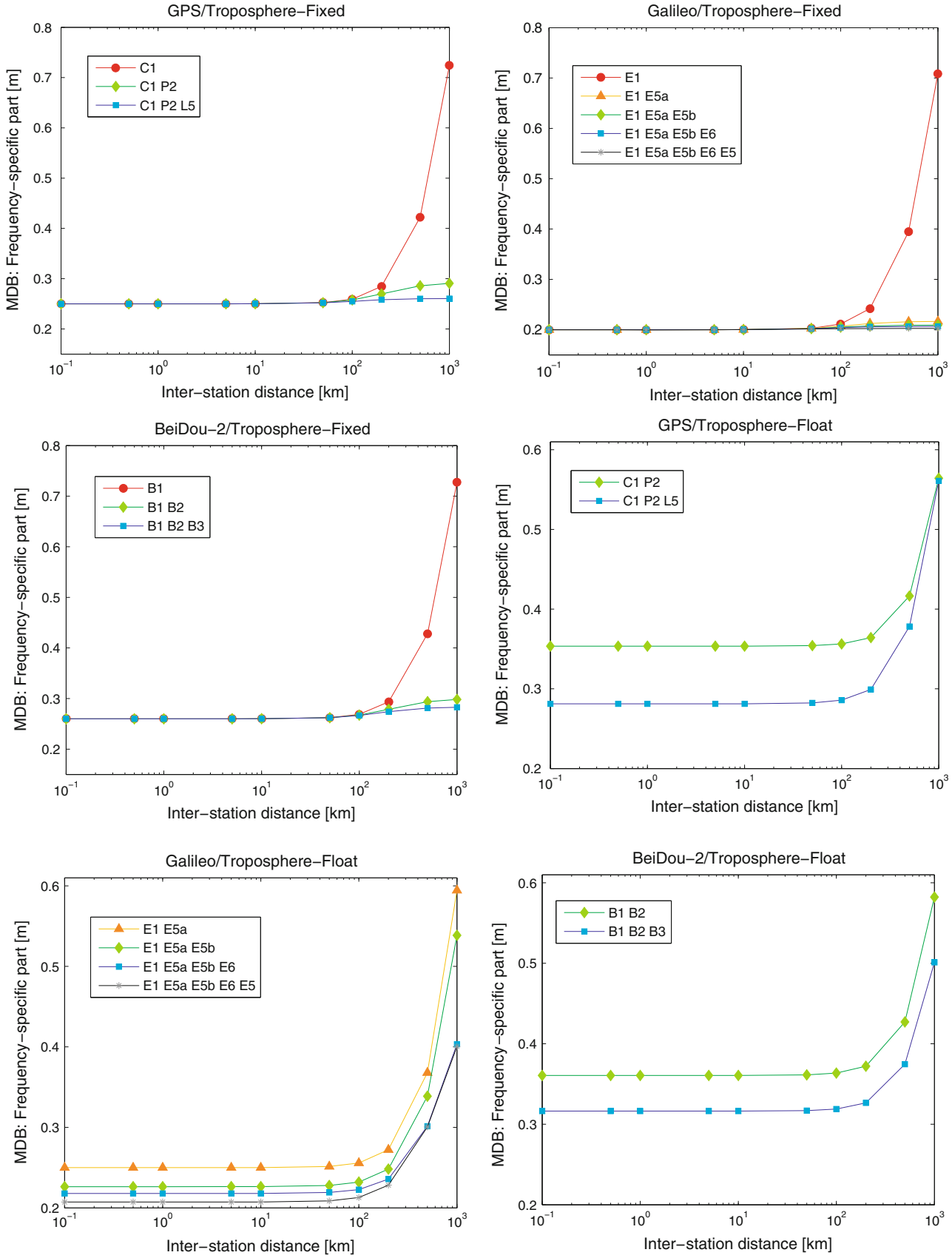

Fig. 2 Frequency-specific part of the code-outlier MDBs [m] as function of the inter-station distance [km] for three GNSSs GPS, Galileo, and BeiDou

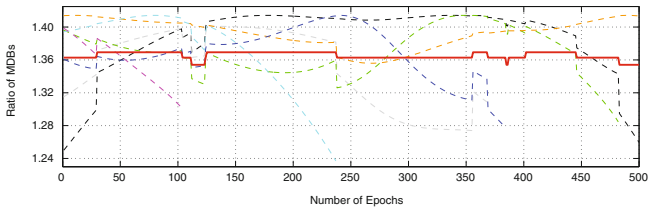

Fig. 3 Reduction-factors (ambiguity-float) of the code-outlier MDB (*dashed lines*) due to mapping the slant tropospheric delays (STDs) to their zenith counterparts (ZTDs) compared to the *rule-of-thumb* formula (*red thick line*) over time (a GPS data-set). Different colors have been used for different satellites

Similar to the satellite-specific part, as the model gets stronger (i.e. $\sigma^2_{\hat{p}_j} \approx 0$), one can only consider the quality of that individual observable-type on frequency j (i.e. $\sigma^2_{p_j}$). As an example, for an array of 4 antennas with the probability of false alarm $\alpha = 0.01$, the code-outlier MDB is about 79 [cm] ($\gamma = 0.8$) and 89 [cm] ($\gamma = 0.9$). In case of phase-slip MDB of two successive epochs, the MDB is about 3.9 [mm] ($\gamma = 0.8$) and 4.4 [mm] ($\gamma = 0.9$). The zenith-referenced standard deviations of the pseudo-range and carrier-phase observables are, respectively, set to $\sigma_{p_j} = 20$ [cm] and $\sigma_{\phi_j} = 1$ [mm].

3.2.1 MDB Reduction-Factor: From the STD-Based Model to the ZTD-Based Model

As stated so far, the MDB given in (17) refers to the STD-based model. One can now ask to what extent the MDB decreases by mapping the STDs to their ZTDs. Following the same procedure as before, the MDB of the ZTD-based model can be formulated that reveals the gain in terms of the reduction of the MDB. Although in addition to the number of frequencies/satellites, the stated reduction-factor does also depend on the tropospheric mapping functions g and the elevation-dependent weight matrix W_s (see Fig. 3), one can however present a *rule-of-thumb* expression as its rough value, namely (ionosphere-fixed scenario)

$$\begin{aligned} &\textit{Before ambiguity-fixing} \\ &\frac{||vec[\nabla]||_{STD}}{||vec[\nabla]||_{ZTD}} \approx [1 + \tfrac{1}{f-1}(\tfrac{s-2}{s-1})]^{\frac{1}{2}} \\ &\textit{After ambiguity-fixing} \\ &\frac{||vec[\nabla]||_{STD}}{||vec[\nabla]||_{ZTD}} \approx 1 \end{aligned} \tag{19}$$

According to the above equations, before fixing ambiguities the reduction-factor is mostly governed by the number of frequencies f but not too much by the number satellites s. As the number frequency increases, the gain in terms of MDB reduction gets less. After fixing ambiguities, the reduction-factor becomes almost 1 meaning that the code-outlier MDB remains almost unchanged by even strengthening the model through mapping the tropospheric delays to their ZTDs.

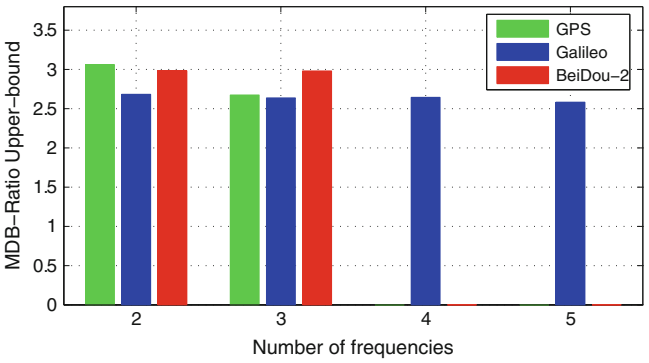

Fig. 4 Upper bounds of the reduction-factor of the ionospheric MDB due to excluding zenith tropospheric delays (ZTDs) from the underlying model for three GNSSs GPS (*green bars*), Galileo (*blue bars*), and BeiDou (*red bars*)

3.3 Atmospheric Detectors and Their MDBs

In most applications dealing with the small-scale arrays, one needs to check as to whether there are significant dispersive/nondispersive effects or not. Taking the atmosphere-fixed scenario as the null hypothesis, the atmospheric detectors are defined as

$$\begin{aligned} &\textit{tropospheric-detector: } C_f \mapsto e_f,\ C_s \mapsto g, \quad C_n \mapsto D_n \\ &\textit{ionospheric-detector: } \ C_f \mapsto \mu, \ C_s \mapsto D_s, C_n \mapsto D_n \end{aligned} \tag{20}$$

Despite the complexity of the atmospheric MDBs, we can evaluate them in a *relative* sense. For instance, one can analyze the reduction of the ionospheric MDB when the differential ZTDs are assumed to be a-priori known via the following bounds (codeless data)

$$1 \leq \frac{||vec[\nabla]||_\tau}{||vec[\nabla]||} \leq [1 + \frac{\bar{\mu}^2}{\sigma^2_\mu}]^{\frac{1}{2}} \tag{21}$$

with $\bar{\mu} = (1/f)\sum_{j=1}^{f} \mu_j$ and $\sigma^2_\mu = (1/f)\sum_{j=1}^{f}(\mu_j - \bar{\mu})^2$. The ionospheric MDBs with and without ZTDs are denoted by $||vec[\nabla]||_\tau$ and $||vec[\nabla]||$, respectively.

According to (21), the detectability of the differential ionosphere can get better at most $[1 + (\bar{\mu}/\sigma_\mu)^2]^{\frac{1}{2}}$ times, if one excludes the differential ZTDs from the model. For the current systems, the stated value is around 3 (cf. Fig. 4).

4 Concluding Remarks

In this contribution, the UMPI test-statistics as well as their MDBs, associated with the array model, were studied. With the aid of the GNSS decoupled misclosures, a few impor-

tant examples such as the array-detector, w-test-statistic and the ionospheric-detector were discussed. In particular, we showed that as the model gets stronger, one can simply, in case of outlier's MDB, analyze the single-channel/frequency scenario instead.

Acknowledgements P.J.G. Teunissen is the recipient of an Australian Research Council Federation Fellowship (project number FF0883188).

Appendix

Proof of (3) The model's misclosures, forming the condition equations, can be formulated through pre-multiplying the corresponding observation vector by an orthogonal complement basis matrix of the design matrix (Teunissen 2000). In case of the single-epoch ambiguity-float scenario, the carrier-phase observations are all reserved to determine the DD ambiguities, thus leaving the code observations to contribute to the redundancy of the model. Given the observations Eq. (1), the code-only design matrix A, together with its orthogonal complement basis matrix B, can therefore be expressed as (per baseline)

$$\begin{aligned} A \mapsto [\, e_f \otimes D_s^T g \;,\; \mu \otimes I_{s-1}\,] \Rightarrow \\ B^T \mapsto \begin{bmatrix} (D_f^T \mu)^{\perp T} D_f^T \otimes c_{d|\tau}^2 g^T D_s (D_s^T W_s^{-1} D_s)^{-1} \\ \mu^{\perp T} \otimes (D_s^T g)^{\perp T} \end{bmatrix} \end{aligned} \tag{22}$$

from which (3) follows. That the misclosures M_1 and M_2 are mutually uncorrelated follows from the identities $D_s^T \bar{g} = D_s^T g$, and $(D_s^T g)^{\perp T} D_s^T g = 0$. □

Proof of Theorem 1 Equation (6) is indeed another expression of the UMPI test-statistic T_q presented in Teunissen (2000). In terms of the model's misclosures M, T_q and its MDB-squared $||\nabla||^2$ read

$$T_q = \frac{1}{q} M^T Q_{MM}^{-1} P_{C_M} M \tag{23}$$

$$||\nabla||^2 = \frac{\nu_{q,\alpha,\gamma}}{d_Y^T C_M^T Q_{MM}^{-1} C_M d_Y} \tag{24}$$

To complete the proof, we thus need to show

$$\begin{aligned} &tr(Q_{MM}^{-1} P_{C_M} M M^T) = M^T Q_{MM}^{-1} P_{C_M} M, \\ &tr(P_{C_M}) = q \end{aligned} \tag{25}$$

The first expression follows from the trace-property $tr(UV) = tr(VU)$ for any matrices U and V of an appropriate size, and the fact that the trace of a scalar is equal to the scalar itself. The second expression follows from the equality between the trace of a projector and its rank, that is

$$tr(P_{C_M}) = rank(P_{C_M}) = q, \tag{26}$$

since $rank(C_M) = q$. □

Proof of (12) In case of the atmosphere-fixed scenario, no differential atmospheric delays are to be estimated, i.e. $\mu = 0$ and $g = 0$. This yields $\mu^\perp = I_f$ and $(D_s^T g)^\perp = I_{s-1}$. According to (3), the frequency-difference misclosures M_1 vanishes, and the vectorized version of the atmosphere-free misclosures M_2 takes the following form

$$M_{\tilde{p}} = [D_n^T \otimes I_f \otimes D_s^T] vec[\tilde{P}] \tag{27}$$

with the variance matrix (cf. (2))

$$Q_{M_{\tilde{p}} M_{\tilde{p}}} = D_n^T D_n \otimes Q_p \otimes D_s^T W_s^{-1} D_s \tag{28}$$

Upon choosing the array-detector structure (11), matrix C_M of $M_{\tilde{p}}$, introduced in Theorem 1, reads then

$$C_{M_{\tilde{p}}} = D_n^T D_n \otimes I_f \otimes D_s^T D_s \tag{29}$$

Similar expressions are formulated for the carrier-phase observations $\tilde{\Phi}$, in case the ambiguities are fixed to their integers. The structures of $M_{\tilde{\phi}}$, $Q_{M_{\tilde{\phi}} M_{\tilde{\phi}}}$ and $C_{M_{\tilde{p}}}$ are thus identical to those of $\tilde{P}$. Substituting $M = [M_{\tilde{p}}^T, M_{\tilde{\phi}}^T]^T$,

$$Q_{MM} = \begin{bmatrix} Q_{M_{\tilde{p}} M_{\tilde{p}}} & 0 \\ 0 & Q_{M_{\tilde{\phi}} M_{\tilde{\phi}}} \end{bmatrix}, \quad C_M = \begin{bmatrix} C_{M_{\tilde{p}}} & 0 \\ 0 & C_{M_{\tilde{\phi}}} \end{bmatrix}, \tag{30}$$

an application of Theorem 1 gives (cf. (6))

$$T_q = \frac{tr\{Q_{M_{\tilde{p}} M_{\tilde{p}}}^{-1} P_{C_{M_{\tilde{p}}}} M_{\tilde{p}} M_{\tilde{p}}^T\} + tr\{Q_{M_{\tilde{\phi}} M_{\tilde{\phi}}}^{-1} P_{C_{M_{\tilde{\phi}}}} M_{\tilde{\phi}} M_{\tilde{\phi}}^T\}}{tr\{P_{C_{M_{\tilde{p}}}}\} + tr\{P_{C_{M_{\tilde{\phi}}}}\}} \tag{31}$$

The proof follows then from

$$P_{C_{M_{\tilde{\phi}}}} = P_{C_{M_{\tilde{p}}}} = I_{n-1} \otimes I_f \otimes I_{s-1}, \tag{32}$$

and

$$\begin{aligned} tr\{Q_{M_{\tilde{p}} M_{\tilde{p}}}^{-1} M_{\tilde{p}} M_{\tilde{p}}^T\} &= tr\{[Q_p^{-1} \otimes W_s P_{e_s}^\perp]\, \tilde{P} P_{D_n} \tilde{P}^T\}, \\ tr\{Q_{M_{\tilde{\phi}} M_{\tilde{\phi}}}^{-1} M_{\tilde{\phi}} M_{\tilde{\phi}}^T\} &= tr\{[Q_\phi^{-1} \otimes W_s P_{e_s}^\perp]\, \tilde{\Phi} P_{D_n} \tilde{\Phi}^T\} \end{aligned} \tag{33}$$

with the projectors $P_{e_s}^\perp = W_s^{-1} D_s (D_s^T W_s^{-1} D_s)^{-1} D_s^T$, and $P_{D_n} = D_n (D_n^T D_n)^{-1} D_n^T$.

The proof of (14), (17), (19) and (21) goes along the same lines as the proof of (12). □

References

Arnold SF (1981) The theory of linear models and multivariate analysis, vol 2. Wiley, New York

Baarda W (1968) A testing procedure for use in geodetic networks. Technical Report, Publications on Geodesy, New Series, vol 2, no. 5. Netherlands Geodetic Commission, Delft

Euler HJ, Goad CC (1991) On optimal filtering of GPS dual frequency observations without using orbit information. J Geod 65(2):130–143

Giorgi G, Henkel P, Gunther C (2012) Testing of a statistical approach for local ionospheric disturbances detection. In: Proceedings of the IEEE-ION Position Location and Navigation Symp (PLANS), 2012. IEEE, USA, pp 167–173

de Jonge PJ (1998) A processing strategy for the application of the GPS in networks. PhD Thesis, Publication on Geodesy, 46, Delft University of Technology, Netherlands Geodetic Commission, Delft

Khanafseh S, Pullen S, Warburton J (2012) Carrier phase ionospheric gradient ground monitor for GBAS with experimental validation. Navigation 59(1):51–60

Odijk D, Teunissen PJG, Khodabandeh A (2014) Single-frequency PPP-RTK: theory and experimental results. IAG Symp 139:167–173

Schaffrin B, Bock Y (1988) A unified scheme for processing GPS dual-band phase observations. Bull Géod 62(2):142–160

Teunissen PJG (1997) GPS double difference statistics: with and without using satellite geometry. J Geod 71(3):137–148

Teunissen PJG (1998) Minimal detectable biases of GPS data. J Geod 72(4):236–244

Teunissen PJG (2000) Testing theory: an introduction. Series on Mathematical Geodesy and Positioning. Delft University Press, Delft

Teunissen PJG (2010) Integer least-squares theory for the GNSS compass. J Geod 84(7):433–447

Teunissen PJG (2012) A-PPP: Array-aided precise point positioning with global navigation satellite systems. IEEE Trans Signal Process 60(6):2870–2881

Teunissen PJG, de Bakker PF (2012) Single-receiver single-channel multi-frequency GNSS integrity: outliers, slips, and ionospheric disturbances. J Geod 87(2):161–177